Journal of Electroanalytical Chemistry 844 (2019) 155–160

Contents lists available at ScienceDirect

Journal of Electroanalytical Chemistry

journal homepage: www.elsevier.com/locate/jelechem

Cathode plasma electrolysis in diluted potassium hydroxide solutions: Particles formation and energetic estimation

Alexander Gromov[a,b,*], Anton Nalivaiko[a], Thomas Fehn[b], Dewi Puspa Muhammad Yahya[b], Alexandra Osipenkova[a], Andreas Koleczko[c], Sebastian Knapp[c], Ulrich Teipel[b]

[a] National University of Science and Technology MISiS, Moscow, Russia
[b] Georg Simon Ohm Technical University, Nuremberg, Germany
[c] Fraunhofer Institute of Chemical Technology, Pfinztal, Germany

ARTICLE INFO

Keywords:
Plasma electrolysis
Particles production
Energy estimation

ABSTRACT

This paper studies production of micron-sized metal particles by plasma electrolysis (PE) using an electrolytic cell with DC current up to 3 A and voltage up to 300 V. A formation of hydrogen plasma on a cathode resulted in electrodes erosion. The PE method was used for the micron-sized metal particles production and potassium hydroxide was used as an electrolyte. The experiments were carried out with different concentrations of KOH (0.125–0.625 wt%). We investigated KOH concentration on the PE regime and, thus, on the size distribution of particles obtained from the plasma-eroded cathode. Particles obtained by PE were comprehensively analysed; particle size distribution curves for powders obtained in different conditions were compared. Particle size distribution curves were shifted to the nano-range with an increased plasma current (KOH concentration). Qualitative energetic estimation of the PE was executed for the open electrolytic cell. Energy balance was used to determine the amount of energy released by the PE.

1. Introduction

Micron-sized metal particles with new functional, electronic, magnetic, optical, and structural properties are of high scientific and engineering importance, as well as the particles with new physical properties, catalytic activity, and solubility [1,2]. However, the elaborate production methods for micron-sized metal particles limit their applicability due to their complexity, high cost, and low productivity [3]. In combination with efficient energy production, new methods of micron-sized metal particles production are in high demand in material science, industry and energetics [4,5].

Plasma electrolysis (PE) is a method to synthesize micron-sized metal particles, comprehensively described in [6,7]. It is relatively simple due to its electrical and technological assembling scheme, which is realized on the basis of the Faraday electrolytic cell in alkali, acidic, or salt-water solutions [8]. Normally, the PE regime is observed at the voltage $U > 100$ V. The second condition of PE occurs when the surface of one electrode is larger as compared to another electrode, i.e., when the anode surface is much larger than that of cathode [6–11]. In this case, a smaller electrode's current density could achieve values of 1 A/mm^2, which results in the PE regime. The formation of thin gaseous bubbles and the bright glowing of the burned gas are observed around the electrode. The plasma discharge is accompanied by bright glowing between the surface of the electrode and the electrolyte. The gas discharge exists in the gaseous bubble [6].

A transition from the Faraday electrolysis regime (without glowing and with approximately equal surface of electrodes) to the PE regime is achieved when the electrolyte solution achieves boiling point in the thin (1–3 mm) zone around the smaller electrode [12,13]. At the beginning of electrolysis, the current increased linearly to a certain maximum value with a voltage increase [14,15]. With the further voltage increase, the current sharply drops down, which indicates the beginning of the PE regime [16,17]. It is also visible by the naked eye. The PE regime is accompanied by a whistling sound and some noise at radio wave frequency. The cathode starts to erode rapidly due to plasma discharge, with the particles of the eroded cathode penetrating

Abbreviations: Q, heat, kJ; I, current, A; U, voltage, V; t, duration, s; Cp_{water}, specific heat of water, kJ/(kg·K); Δh_{water}, evaporation heat of water, kJ/kg; T_1, final electrolyte temperature, K; T_2, initial electrolyte temperature, K; m_1, electrolyte weight, kg; m_2, water vapor weight, kg; T_u, ambient temperature, K; T_s, electrolyte temperature, $T_s = T_1$, K; α, heat transfer coefficient, W/(m^2·K); λ, coefficient of thermal conductivity, W/(m·K); s, beaker wall thickness, m; D, beaker diameter, m; l, electrolyte level in a beaker, m

* Corresponding author at: Process Engineering Faculty, Georg Simon Ohm Technical University Nuremberg, 12, Kesslerplatz, 90489 Nuremberg, Germany.
E-mail address: a.gromov@misis.ru (A. Gromov).

https://doi.org/10.1016/j.jelechem.2019.04.065
Received 13 November 2018; Received in revised form 5 April 2019; Accepted 26 April 2019
Available online 09 May 2019
1572-6657/

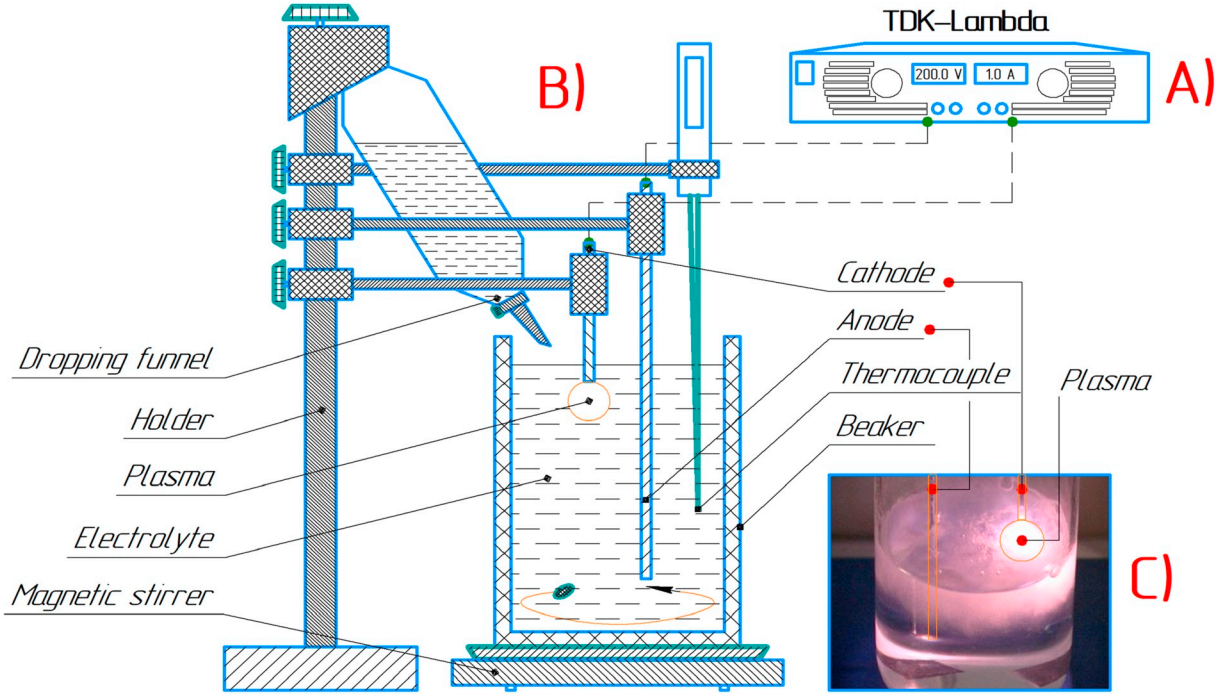

Fig. 1. Lab PE cell: DC power source TDK-Lambda (a), common view (b), in operation (c).

into the water-based electrolyte [18–21].

Our research is aimed to characterize the particles released from the eroded cathode during the PE. We also made an effort to estimate PE's energetic efficiency.

2. Experiment

2.1. Plasma electrolysis

With a laboratory-sized PE cell (Fig. 1) and DC power supply [22], the experiment was conducted using different concentrations of potassium hydroxide (KOH, 99.9 wt% of purity) as an electrolyte in order to observe its effect 1) on micron-sized metal particles production and 2) on the amount of energy introduced and released. Potassium hydroxide (KOH) refers to strong electrolytes and it has a very good water solubility (~55 g per 100 ml of water at 25 °C). Therefore, KOH was chosen as the electrolyte.

The PE cell's detailed image is shown in Fig. 1. In this work, the "cathode-type PE" was studied: the surface of the cathode was smaller in comparison with the anode and, thus, the cathode had much higher current density on its surface. The electrolytic cell was a 400 ml beaker containing electrolyte, and was placed on a magnetic stirring plate because the electrolyte had to be continuously stirred during the experiment to ensure a uniform temperature distribution. Otherwise, the near-cathode field of the electrolyte would heat very fast and would boil while the bottom of the cell would still be cold (see Supplementary materials). The thermal equilibrium inside the electrolytic cell was not achieved in our experiments due to the fast heating process.

The cathode made from stainless steel W2 was placed vertically to a depth of approximately 10 mm below the electrolyte surface (Fig. 1). In all experiments, stainless steel W2 was used as the anode. Electrodes (cathode and anode) were made from wires with the following dimensions:

- anode 2 mm diameter, 250 mm length, 1500 mm^2 working surface;
- cathode 2 mm diameter, 10 mm length (inside electrolyte), 63 mm^2 working surface. The ratio of the surface of anode/cathode is equal to 24.

The volume of the cell's water-based electrolyte gradually decreased during the experiments because of evaporation and boiling. A 250 ml dropping funnel with a valve was attached to the cell. Room temperature water was gradually added to maintain the constant electrolyte level and alkali concentration in the cell. The loss of water-based electrolyte was not more than ~1 wt% during the experiment (60 min). Also, a thermocouple (Ni-CrNi, type K) was immersed into the electrolyte solution and attached to the holder (Fig. 1).

The DC power source used was TDK-Lambda with a voltage in the range from 0 to 300 V and current from 0 to 2.5 A [22]. The measurement error of the electrolysis output parameters (current, voltage) was not more than ± 0.05%. The experiments were carried out at a constant potential. The PE cell scheme is shown in Fig. 2.

Various KOH solution (99.9 wt% of purity) electrolyte concentrations (from 0.125 to 0.625 wt%) were used to determine the PE conditions that resulted in particles obtained by intensive cathode erosion. The aim of the dilute KOH solution application was to study, at the same time, the PE with a minimum amount of elements in water (K, O, and H) and high current achievement. A second aim was to avoid an intensive electrode corrosion by PE and to avoid their fast degradation. The minimal KOH concentration for the PE regime appearance was 0.05 wt%.

The temperature of the glowing plasma cathode was estimated using the known melting point of stainless steel (melting temperature T_m = 1400 °C) as the reference for the thermal balance. We were not able to measure the apparent plasma temperature by spectroscopic methods due to the calibration problem and, thus, we used the melting point of stainless steel as a reference. The temperature of plasma appearance was determined using the thermocouple, so the values are only indicative and were typical for all solution concentrations (~80 °C).

2.2. Particles analysis

The micron-sized metal particles were formed due to the PE process's cathode erosion. During the experiment, the produced particles were kept in the solution and collected for size distribution analysis using a laser diffraction method (HELOS & QUIXEL, Germany).

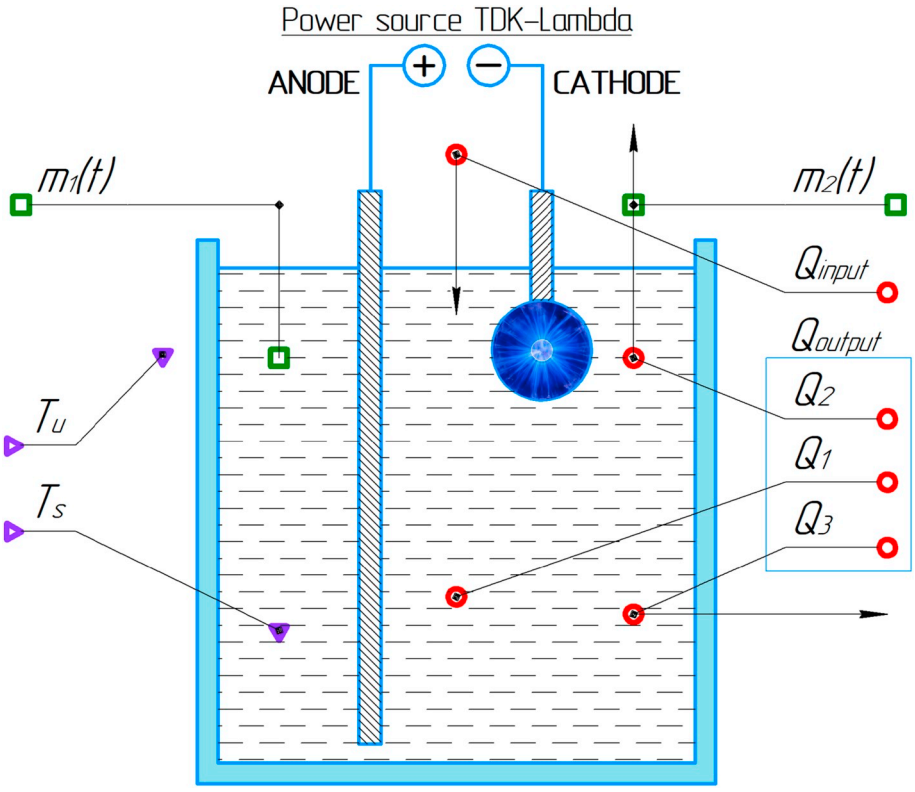

Fig. 2. PE cell scheme with thermodynamic parameters for mass and thermal balance calculation: T_u – ambient temperature; T_s – system temperature; Q_1 – heat, required for heating; Q_2 – heat loss due to evaporation; Q_3 – heat loss via beaker wall; Q_{input} – heat that is introduced into the system; $m_1(t)$ – mass of the electrolyte; $m_2(t)$ – mass of water, which evaporated.

Table 1
Calculated values of heat introduced into the system (Q_{input}) and heat dissipated by the system ($Q_{output} = Q_1 + Q_2 + Q_3$) during PE experiment (see Section 3. Thermodynamic calculations).

KOH concentration, wt%	Heat, kJ					
	Q_{input}	Q_1	Q_2	Q_3	Q_{output}	Q_{input} - Q_{output}
0.125	154	50	89	15	154	0
0.255	178	69	93	16	178	0
0.375	211	96	95	20	211	0
0.500	238	110	106	22	238	0
0.625	241	111	108	22	242	1

Table 2
Conductivity values and change of cathode mass before and after PE at different KOH concentrations.

KOH concentration, wt%	Conductivity, S/m	Mass of cathode change after PE experiment (Δm), wt%
0.125	0.61	−5.3
0.250	1.22	−4.5
0.375	1.83	−8.1
0.500	2.44	−11.1
0.625	3.05	−11.3

The elemental composition of the particles was studied by EDAX TSL, Ametek, USA.

3. Thermodynamic calculations

The PE cell was viewed thermodynamically to calculate the energy balance. These calculations were made using a system balancing analysis as shown in Fig. 2. A closed system model was used for calculation. All thermal flows and relevant substances are shown in Fig. 2. A quantity factor was considered to be able to set the thermal balance. The thermal balance was determined for input and output thermal flows with two formulas [23]:

$$\textit{Input Heat: } Q_{input}\,[J] = I\,[A]\cdot U\,[V]\cdot t\,[s] \quad (1)$$

$$\textit{Output Heat: } Q_{output}\,[J] = Q_1 + Q_2 + Q_3 \quad (2)$$

The input heat comes from the electric power only and, thus, could be easily calculated with the Eq. (1). The output heat (Eq. (2)) consisted of different parts [24]:

$$\textit{Electrolyte Heat: } Q_1[J] = Cp_{water}\cdot m_1(t)\cdot(T_1 - T_0) \quad (3)$$

$$\textit{Evaporation Heat: } Q_2[J] = \Delta h_{water}\cdot m_2(t) \quad (4)$$

$$\textit{Convection Heat: } Q_3[J] = S\cdot(t_1 - t_0)\cdot\left(\frac{T_s - T_u}{\frac{1}{\alpha_{air}} + \frac{s}{\lambda_{glas}} + \frac{1}{\alpha_{water}}}\right) \quad (5)$$

$$\textit{Beaker surface area: } S = D\cdot\pi\cdot l + \frac{1}{4}\cdot\pi\cdot D^2 \quad (6)$$

Q_1 is the energy needed to heat the electrolyte, and this was calculated based on the temperature difference before and after the reaction. Q_2 is the heat used for electrolyte evaporation. Q_3 was considered as the loss of electrolyte heat during its cooling, which occurs due to the temperature gradient of the electrolyte and the environment. The electrolyte dilution was very high, and, thus, the cell thermodynamic properties were comparable to water. That is why the enthalpy of water evaporation was taken for the calculation. The heat loss due to the convection over the PE cell was calculated with Eq. (5). All the calculated values of Q_{input}, Q_1, Q_2, and Q_3 are presented in Table 1. We found that there was 1 kJ of excess heat released with 0.625 wt% KOH and this might refer to the energy dissipation as bright glowing plasma. However, plasma glowing requires a more detailed spectroscopic study.

4. Results and discussion

During PE experiments, the cathode began glowing brightly and the electrolyte around the cathode was boiled, which resulted in the

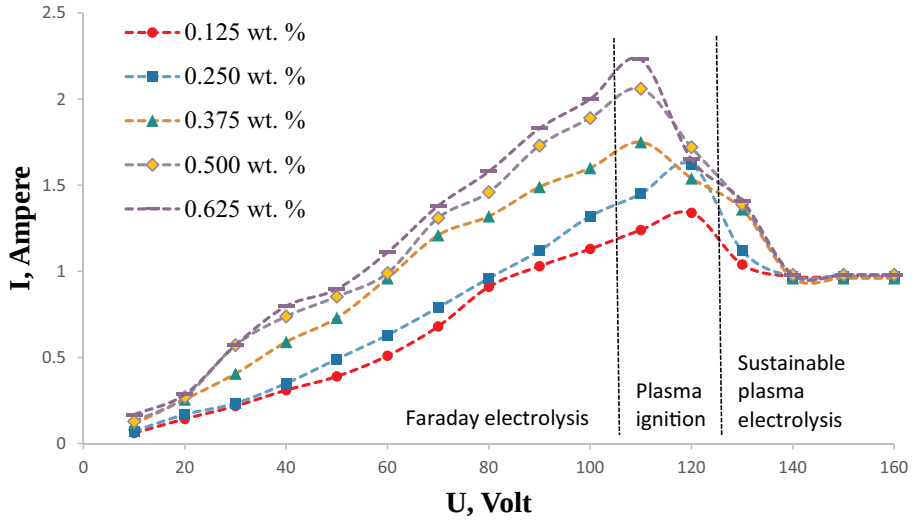

Fig. 3. Volt-Ampere characteristic of PE cell with the stainless steel W2 cathode and the certain values of KOH concentrations (see Table 2).

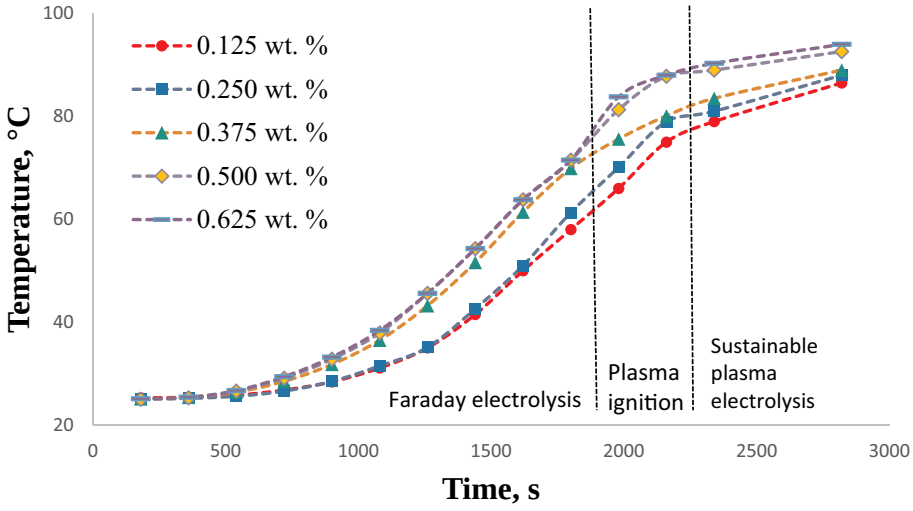

Fig. 4. Temperature change of PE cell with the stainless steel W2 cathode at certain values of the concentrations of KOH (see Table 2).

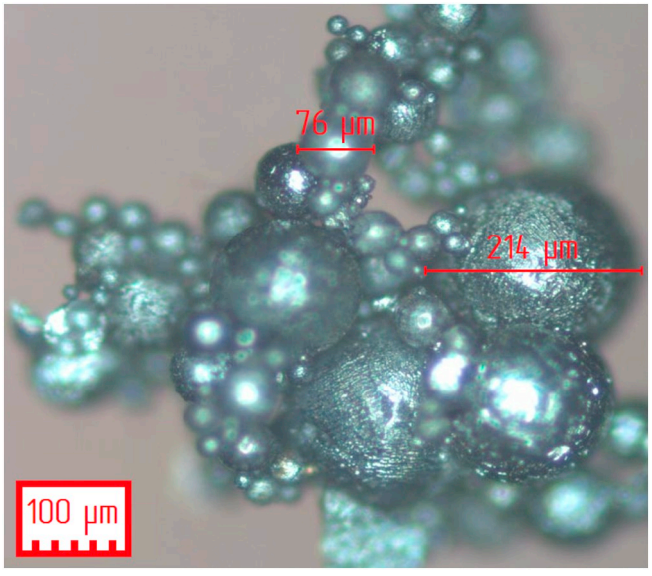

Fig. 5. Optical microscope image of stainless steel particles produced by PE.

formation of gas bubbles surrounding the cathode. This glowing was accompanied by hydrogen burning (the experiment's total duration was about 3000 s). Thus, electrode erosion occurred, which resulted in the production of micron-sized metal particles. The appearance of plasma and the formation of particles occurred simultaneously. The bright glowing referred to the plasma discharge – analogue to "corona" plasma discharge in gases. At low voltage (~110 V) and at the electrolyte concentration of 0.1 wt% of KOH, the colour of glowing, i.e., the colour of plasma discharge, was white-yellowish. With a voltage increase, the plasma colour changed into yellowish-orange (potassium lines).

Conductivities of the used solutions are listed in Table 2, and they are well suited to perform electrolysis. The conductivity increased as expected with KOH concentration increasing. Since the conductivity was high enough, and the current at the corresponding voltage was also high enough, as shown in Fig. 3, the transition region from the Faraday regime to the PE was achieved in a range of voltage values between 110 V and 120 V. The higher the conductivity values, the faster the plasma appearance temperature was reached.

With KOH concentration increasing, the electric current and the cell temperature increased as well (Fig. 4). It can be seen that the final temperatures were different by about 5 °C. This is due to the fact that by the current increasing, the introduced heat (Q_{input}) increased as well.

The cathodes were weighed before and after each experiment to

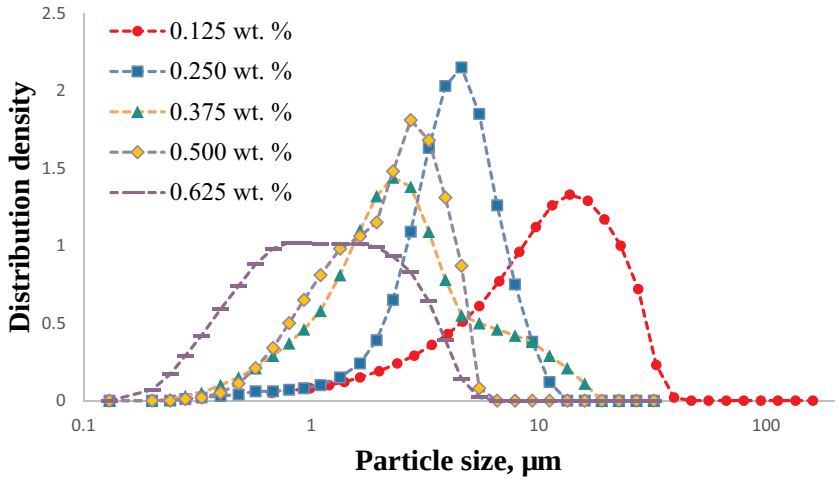

Fig. 6. Size distribution curves of stainless steel particles produced by PE for different KOH concentration.

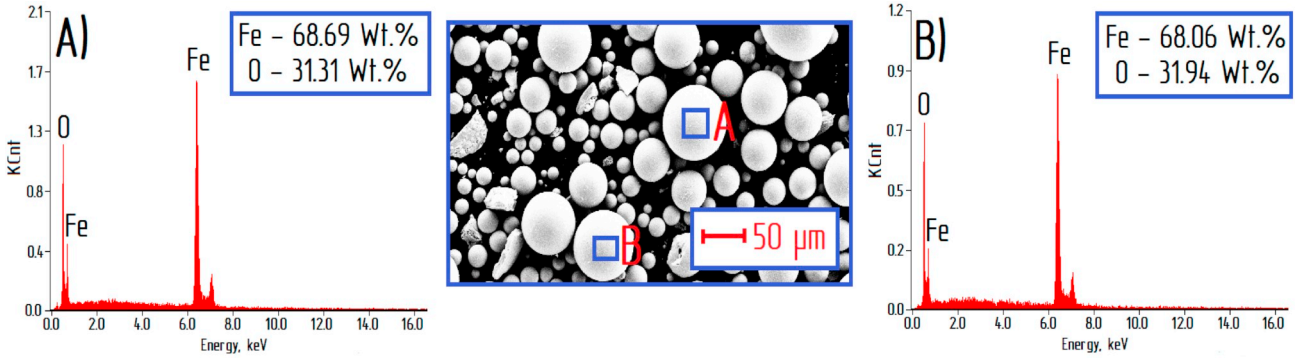

Fig. 7. Elemental composition (left and right patterns) and SEM image with the certain areas A and B of analysis (middle) of the stainless steel W2 particles obtained after PE at KOH concentration 0.125 wt%.

determine the mass of the obtained particles and their percentage in the initial weight of the cathode. After electrolysis, the weight of the cathode decreased, as shown in Table 2, due to both the electrode erosion during PE and the micron-sized metal particles formation (Fig. 5). The Faraday electrolysis regime did not lead to valuable electrodes erosion. Cathode erosion is probably associated with high plasma temperatures and partial melting of the electrode's surface layers. Hydrogen gas also destructed the surface layer of the cathode with the formation of particles, showing that particles chemical oxidation is possible. It is worth noting that cathodic corrosion occurring at variable potential, as described in studies [25–28], is not the dominant process in particle formation and is not observed in plasma electrolysis. Particle formation occurs due to the mechanical action of hydrogen gas and the thermal effect of plasma, that is, erosion. The electrode erosion mechanism is thoroughly discussed in [6].

A prerequisite for the particles production by the PE was that the cathode's generated plasma was hot enough to melt the metal electrode and thus, the particles had a spherical shape typical for the “liquid → solid” mechanism of the particles formation. The analysis of the produced particles size distribution using the laser diffraction is shown in Fig. 6. The higher the electrolyte concentrations, the smaller the size of the formed particles. In the first series of measurements, most of the generated particles were located at approximately 11 μm (maximal content), whereas in the last measurements series, a maximal distribution of 0.7 μm to 2 μm was detected. In the first 4 measurements, only small part particles in the nano–range were generated. An agglomeration of the particles occurred. The plasma was hot enough to produce some part of particles in the nano-ranged sizes.

The elemental composition of the obtained particles is shown in Fig. 7. The particles were washed in distilled water and dried at 150 °C before analysis. Potassium (K) in the particles composition was absent. The main elements were iron (Fe) and oxygen (O). We can conclude, then, that the oxidation occurred by cathode erosion.

5. Conclusions

Cathode plasma electrolysis in the diluted KOH solutions as tested as a method for micron-sized metal particles production. The applied voltage and the relative size of the electrodes, i.e., current density, play important roles in the PE regime. The higher the concentration of the electrolyte used, the smaller the size of the particles that were synthesized by its erosion. So, all the particles were generated in the range of < 500 μm. Surprisingly, PE could also generate many particles in the nano-range (0.4–0.7 μm). The smallest measurable particles were about 0.2 μm. Subsequently, the high current density was responsible for the temperature increase around the cathode, which results in plasma discharge.

The plasma temperature was estimated to be around the melting temperature of the electrodes used; i.e., it was close to the melting temperature of stainless steel (1400 °C). At 0.625 wt% KOH concentration, the excess energy of 1 kJ was found and it might be the result of plasma action. Since it is not possible yet to consider all factors of energy dissipation, the used method of energy equation balancing is only a good approximation for the system.

Supplementary data to this article can be found online at https://doi.org/10.1016/j.jelechem.2019.04.065.

Acknowledgments

The work is financially supported by Russian Scientific Foundation grant № 19-79-30025 and Alexander-von-Humboldt Foundation in frame of the Fellowship for A.A. Gromov.

The authors thank the NUST "MISIS" Academic Writing Centre for its assistance in the preparation of this manuscript.

References

[1] A. Gromov, U. Teipel, Metal Nanopowders: Production, Characterization, and Energetic Applications, Weinheim, Wiley-VCH, Germany, 2014.
[2] D.L. Fedlheim, C.A. Foss, Metal Nanoparticles: Synthesis Characterization and Applications, CRC Press, Boca Raton, FL, USA, 2001.
[3] G. Schmid, Nanoparticles, Wiley VCH (2005).
[4] W. Dingsheng, Li Yadong, Bimetallic nanocrystals: liquid-phase synthesis and catalytic applications, Adv. Mater. 23 (9) (2011) 1044–1060.
[5] N. Shirai, S. Uchida, F. Tochikubo, Synthesis of metal nanoparticles by dual plasma electrolysis using atmospheric dc glow discharge in contact with liquid, Jpn. J. Appl. Phys. 53 (2014) 046202.
[6] M. Aliofkhazraei, A.S. Rouhagdam, Fabrication of Nanostructures by Plasma Electrolysis, Wiley-VCH, Germany, Weinheim, 2009.
[7] T. Mizuno, T. Ohmori, T. Akimoto, Generation of Heat and Products During Plasma Electrolysis, 10th International Conference on Cold Fusion, Cambridge, USA, (2003).
[8] Y. Zongcheng, D. Lihua, Li Ch, Cathodic plasma electrolysis in 1 – propanol solution for preparation of submicron diamond particles, Electrochim. Acta 105 (2013) 612–617.
[9] J. Wu, L. Fan, L. Dong, J. Deng, et al., Cathodic plasma electrolysis for preparation of diamond-like carbon particles in glycerol solution, Mater. Chem. Phys. 199 (2017) 289–294.
[10] N. Sharma, G. Diaz, E. Leal-Quiros, Evaluation of contact glow-discharge electrolysis as a viable method for steam generation, Electrochim. Acta 108 (2013) 330–336.
[11] J. Wu, B. Wang, Y. Zhang, R. Liu, et al., Enhanced wear and corrosion resistance of plasma electrolytic carburized layer on T8 carbon steel, Mater. Chem. Phys. 171 (2016) 50–56.
[12] A. Allagui, E.A. Baranova, R. Wütherich, Synthesis of Ni and Pt nanomaterials by cathodic contact glow discharge electrolysis in acidic and alkaline media, Electrochim. Acta 93 (2013) 137–141.
[13] S.K. Sen Gupta, Contact glow discharge electrolysis: a novel tool for manifold applications, Plasma Chem. Plasma Process. 37 (4) (2017) 897–945.
[14] A.I. Maksimov, A.V. Khlustova, Low-voltage underwater electric discharges: physical properties and application possibilities, Plasma Phys. Rep. 39 (13) (2013) 1099–1103.
[15] A.L. Yerokhina, X. Nie, A. Leyland, A. Matthews, S.J. Dowey, Plasma electrolysis for surface engineering, Surf. Coat. Technol. 122 (2–3) (1999) 73–93.
[16] Jinzhang Gao, Jie Yu, Yan Li, Xiaoyan He, Lili Bo, Lumei Pu, Wu Yang, Quanfang Lu, Zhiming Yang, Decoloration of aqueous Brilliant Green by using glow discharge electrolysis, J. Hazard. Mater. (2006) 431–436 B137.
[17] Y. Zhang, X. Jin, Y. Wang, et al., Effects of experimental parameters on phenol degradation by cathodic microarc plasma electrolysis, Sep. Purif. Technol. 201 (2018) 179–185.
[18] Z. Wu, Z.K. Zhang, D.Z. Guo, Titanium dioxide nanospheres with wide spectral absorption prepared by low-voltage plasma electrolysis, J. Colloid Interface Sci. 392 (2013) 463–464.
[19] M. Aliofkhazraei, A.S. Rouhaghdam, P. Gupta, Nano-fabrication by cathodic plasma electrolysis, Crit. Rev. Solid State Mater. Sci. 36 (3) (2011) 174–190.
[20] T. Mizuno, T. Ohmori, T. Akimoto, A. Takahashi, Production of heat during plasma electrolysis in liquid, Jpn. J. Appl. Phys. 39 (2000) 6055–6061.
[21] T. Abdul Kareem, A. Anu Kaliani, Glow discharge plasma electrolysis for nanoparticles synthesis, Ionics 18 (2012) 315–327.
[22] TDK-Lambda Germany GmbH, Genesys, Programmable DC Power Supplies, Data Sheet, Karl-Bold-Str. 40, D-77855 Achern, Germany, (2008).
[23] Peter W. Atkins, Julio de Paula, Physikalische Chemie, 5. Aktualisierte Auflage, (2013).
[24] Hickling A. Electrochemical processes in glow discharge at the gas-solution interface, Modern Aspects of Electrochemistry, ed. by J. O.M. Bockris and B. E. Conway, Plenum Press New York (1971) 329–373 (No. 6).
[25] B.N. Kabanov, I.I. Astakhov, I.G. Kiseleva, Formation of crystalline intermetallic compounds and solid solutions in electrochemical incorporation of metals into cathodes, Electrochim. Acta 24 (1979) 167–171.
[26] A.I. Yanson, et al., Cathodic corrosion: a quick, clean, and versatile method for the synthesis of metallic nanoparticles, Angew. Chemie Int. Ed. 50 (2011) 6346–6350.
[27] T.J.P. Hersbach, et al., Alkali metal cation effects in structuring Pt, Rh, and Au surfaces through cathodic corrosion, ACS Appl. Mater. Interfaces 10 (2018) 39363–39379.
[28] M.J. Lawrence, et al., Electrochemical synthesis of nanostructured metal-doped titanates and investigation of their activity as oxygen evolution photoanodes, ACS Appl. Energy Mater. 1 (2018) 5233–5244.